# Nanolithography by non-contact AFM-induced local oxidation: fabrication of tunnelling barriers suitable for single-electron devices

**B Irmer, M Kehrle, H Lorenz and J P Kotthaus**

Sektion Physik, Ludwig-Maximilians Universität München, 80539 München, Germany

**Abstract.** We study local oxidation induced by dynamic atomic force microscopy (AFM), commonly called tapping mode AFM. This minimizes the field-induced forces, which cause the tip to blunt, and enables us to use very fine tips. We are able to fabricate Ti–TiO$_x$ line grids with 18 nm period and well-defined isolating barriers as small as 15 nm. These junctions show a non-linear current–voltage characteristic and an exponential dependence of the conductance on the oxide width, indicating tunnelling as the dominant conduction mechanism. From the conductance–barrier width dependence we derive a barrier height of $\Phi = 178$ meV. Numerical calculations of the lateral field distribution for different tip geometries allow us to design the optimum tip for the most localized electric field. The electron beam deposition technique makes it possible to produce tips of the desired geometry.

Proximal probe based lithography has developed over recent years into a well-established tool for the fabrication of structures and electronic devices with nanometric dimensions. In particular, the tip-induced oxidation or, more generally, tip-induced local chemical reactions have been very successful [1–5] and appear to be one of the most promising approaches: they preserve the high lateral resolution of the scanned tip by omitting a subsequent etching step and thus avoid the problem of transferring the pattern into an underlying electron system, e.g. metallic thin films or heterostructures. Furthermore, this approach enables one to monitor the process *in situ* by measuring electronic properties, e.g. the conductance of a thin channel, defined and constricted by atomic force microscopy (AFM) induced oxide [6], or the formation of a barrier across a conducting channel [7]. To use this process optimally in nanofabrication requires (1) the understanding of the underlying electrochemical mechanism and the parameters that control it, (2) a tip, which is optimized for laterally focusing the electric field strength under the experimental conditions, and (3) a scanning technique which allows one to use these tips and to retain their properties. Here, we show that operating the atomic force microscope in a dynamic, non-contact mode is suitable for inducing local oxidation. Hereby the damage to the tip is reduced significantly and it allows us to address questions involving the importance of the tip radius and the overall geometry of the tip.

We start with thermally oxidized (250 nm SiO$_2$) n-type (10 $\Omega$ cm) Si (100) material, on top of which 30–50 Å titanium is thermally evaporated at high evaporation rates ($\approx$10 Å s$^{-1}$) and low background pressure ($p \leq 10^{-8}$ mbar). This metallic film is then patterned using optical lithography and an HF wet etch and finally wire bonded. Local oxidation is performed using a commercial atomic force microscope (Digital Instruments) and highly doped n$^+$-Si tips (NanoSensors), which we further sharpen by oxidation. Tip radii are well below 100 Å, typically around 50 Å. The relative humidity is kept constant at 40% during experiments shown here. The cantilever oscillates near its resonance frequency (approximately 250 kHz) with high amplitudes (10–100 nm). The applied tip bias for local oxidation induces additional charges on the tip, which bends the cantilever towards the surface. This force adds to the normal loading force and can easily damage either the tip or the surface. Moreover, in dynamic AFM the force gradient $\partial F/\partial z$ due to the electric field changes the force constant $k$ to $k^\star = k - \partial F/\partial z$, shifting the resonance frequency to $\omega_0^\star = (k^\star/m)^{1/2}$. The driving bimorph oscillates unchanged at the fixed frequency $\omega < \omega_0^\star < \omega_0$, and therefore the oscillation amplitude is increased. The change in amplitude for a given tip bias can be easily measured from amplitude versus distance curves, which then can be used to readjust the working setpoint. As the feedback is enabled all the time and the damping of the amplitude does not change if only the setpoint is readjusted, the overall loading force
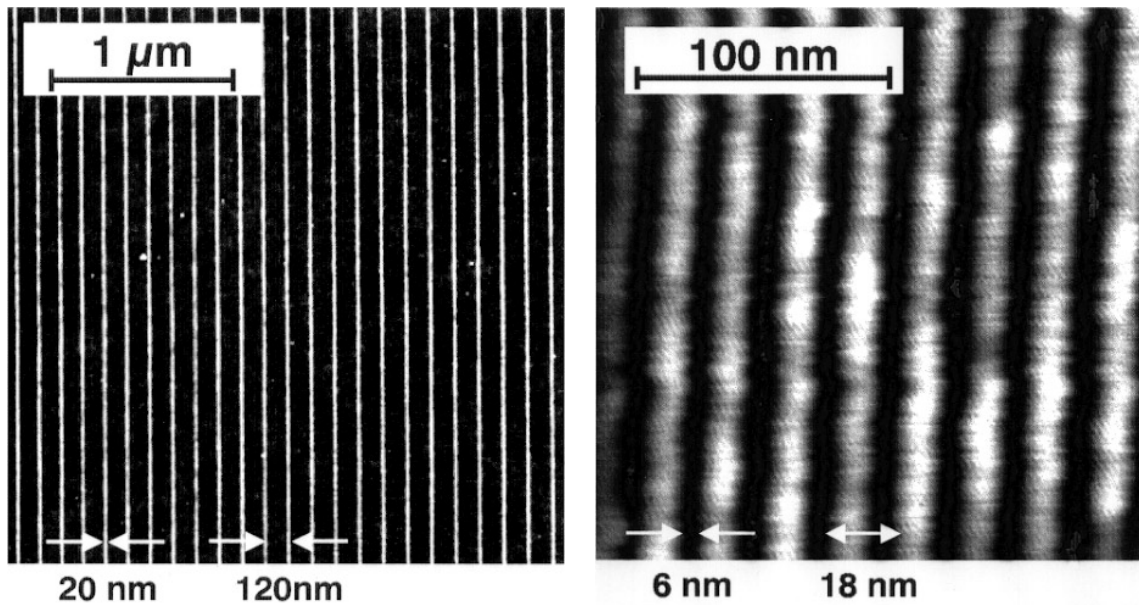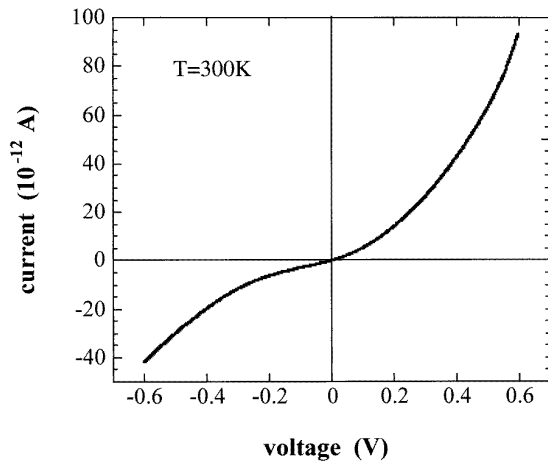
**Figure 1.** Two Ti–TiO$_x$ grids written by tapping mode AFM-induced local oxidation at −6.5 V tip bias and a scan speed of 300 nm s$^{-1}$. At room temperature, the resistance parallel to the lines is 100 kΩ and perpendicular to them ≫80 MΩ.
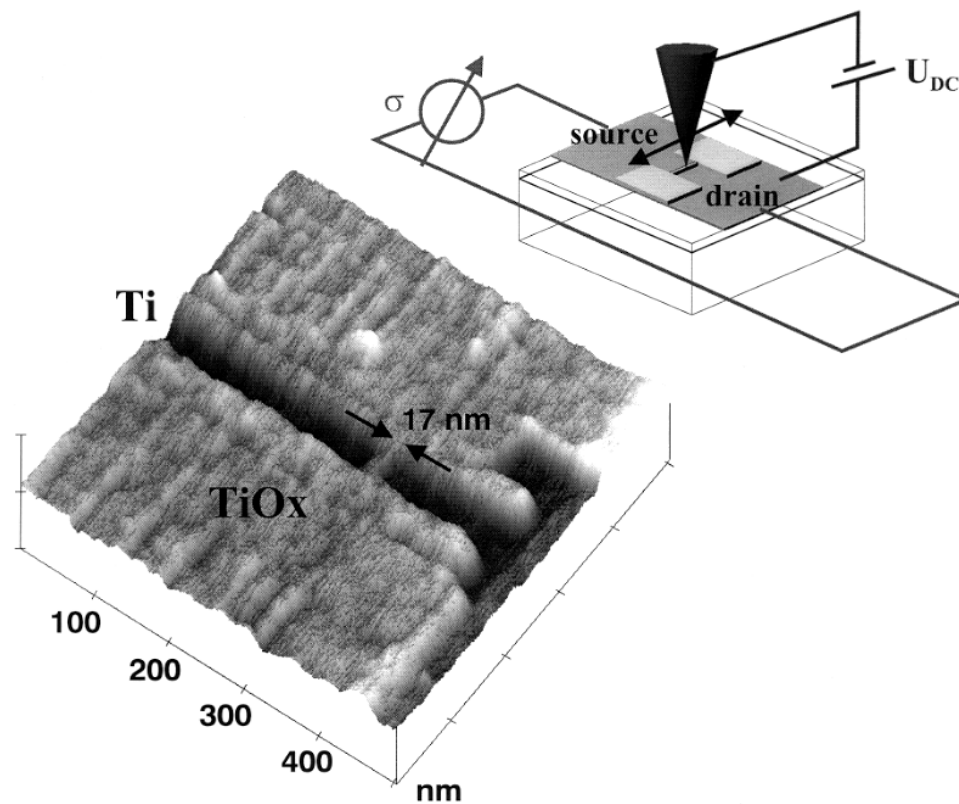


**Figure 2.** *In situ* control of the barrier formation. The source–drain conductance through the device is monitored while oxidizing. The tip is biased at −4 V and repeatedly scanned at 2 Hz across the 30 nm wide Ti channel to form a 17 nm wide barrier.

remains unchanged even for applied voltages up to 30 V [7]. In figure 1 we show two grids of oxide lines written at a rate of 300 nm s$^{-1}$ at a tip bias of −6.5 V. The lines are very regular in width (18–20 nm) as well as in height,

even for relatively large scan fields of 3 mm × 3 mm and above. If the period is reduced from 120 nm to 23 nm, parallel conducting wires of 6 nm linewidth are formed, which are still conductive along the channels (≈100 kΩ)
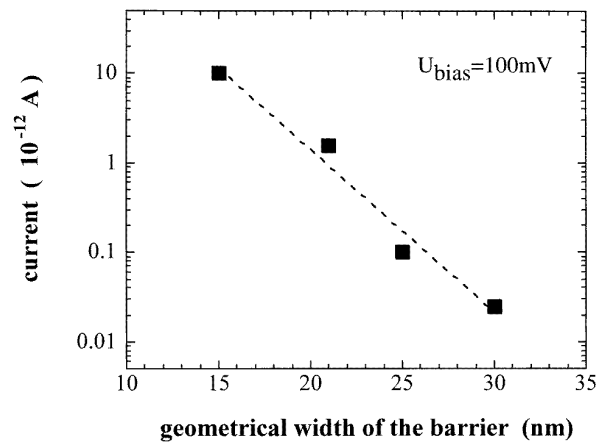
**Figure 3.** Room temperature current–voltage characteristic of a 20 nm wide barrier.



**Figure 4.** Dependence of the current on the geometrical barrier width. Four different devices are measured at 100 mV bias and $T = 300$ K. The current depends exponentially on the barrier width, indicating tunnelling as the dominant conduction mechanism.

but isolating in the perpendicular direction ($\gg 80$ M$\Omega$, at room temperature). This demonstrates a complete oxidation process for the most of the average of the oxide lines. The observed oxide height is 3 nm, which agrees very well with what is expected from the change in density and molecular weight: $d_{TiO_2}/d_{Ti} = (\rho_{Ti}/\rho_{TiO_2})M_{TiO_2}/M_{Ti} \approx 3$ nm/5 nm. It should be noted that, at a tapping frequency of $f_T = 250$ kHz and the observed damping of the amplitude, the contact time $t = 1/2f_T$ between the tip and the sample surface per cycle is below $10^{-3}$ ms. As the oscillation amplitude is very large (10–100 nm), it is unlikely that a stable water meniscus forms between tip and sample. Evidence for this is provided by force versus distance curves in contact AFM using the same cantilevers (data not shown). If the experiment is to be explained in a classical electrochemical set-up, wherein the tip acts as cathode, the water film as electrolyte and the sample as anode, the total exposure time is much shorter than in contact AFM. However, the total amount of oxidized material is very much the same as seen by contact AFM, e.g. by Avouris *et al* [8] for Si or by Sugimura *et al* [9] for Ti. We therefore conclude that corrosion has taken place at the Ti–TiO$_x$ interface, enhanced by the tip–sample electric field in the presence of humidity.

To define a tunnelling barrier we first constrict a predefined 1 mm Ti wire by oxidizing two large oxide pads, enclosing a 30 nm wide channel (figure 2). The barrier, perpendicular to the channel, is then oxidized at 2 Hz scanning frequency and a tip bias of $-4.5$ V. In order to avoid the formation of too thick barriers with a too small tunnelling probability by overexposure, we monitor the conductance along the channel. As soon as the conductance drops below the capacitive signal, oxidation is stopped. The quality of the AFM-induced oxide is characterized on wide barriers ($\approx 100$ nm). Resistivities of $\rho = 2 \times 10^{11}$ $\Omega$ cm and maximum field strength $V_D = 2 \times 10^6$ V cm$^{-1}$ are measured. These values are similar to those for macroscopic anodic oxides [10, 11].

At room temperature the devices show an asymmetric, non-linear $I$–$V$ characteristic (figure 3). This may be understood in the picture of an asymmetrical, shallow
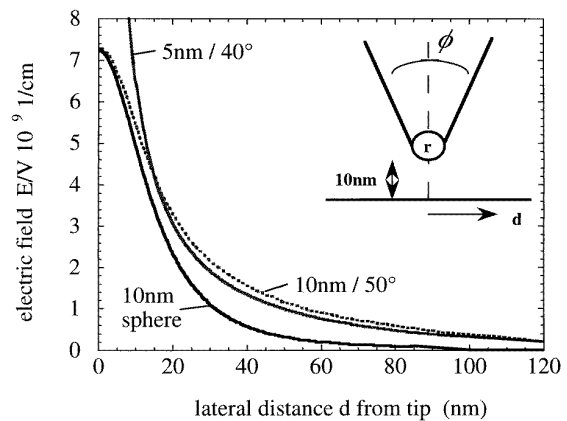


**Figure 5.** Calculated electric field distribution for three tips with different $(r, \phi)$ geometries, 10 nm in front of a conductive plane in vacuum: 10 nm sphere and pyramidal tips with 10 nm radius and 50° cone angle and 5 nm radius and 40° cone angle.

barrier, which is no longer isotropic for forward and reverse biases. To determine the conduction mechanism for these devices, we investigate the dependence of the (tunnelling) current on the geometrical width of the barrier as obtained from AFM images. For four different devices, with barriers varying from 15 nm to 30 nm, the current decays exponentially with barrier width, indicating tunnelling as the dominant conduction mechanism (figure 4). We obtain here a barrier height of $\Phi = 178$ meV.

To determine the parameters that affect the lateral resolution of the oxidation and therefore to estimate the ultimate limit for this technique, we model the lateral field distribution for different tip geometries, namely tip radii and cone angles. In a first step we place the tip 10 nm in front of a conducting surface. The calculated electric field for a 10 nm sphere (radius in each case), a 10 nm spherical tip with 50° pyramidal cone and a 5 nm spherical tip with 40° cone are shown in figure 5. As expected, the pyramids widen the lateral field compared with the free-
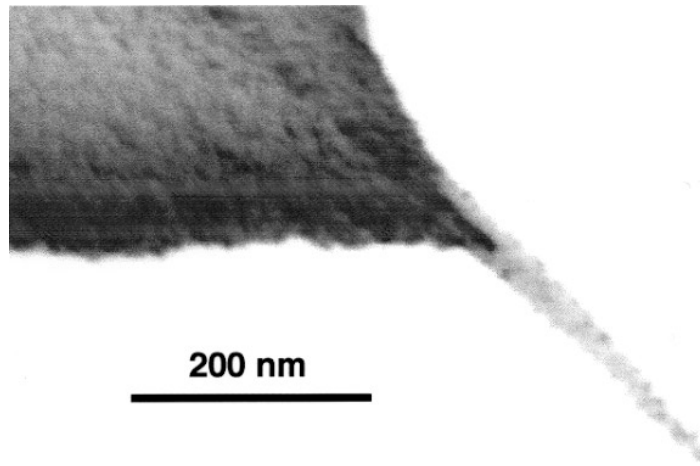
**Figure 6.** SEM image of an EBD tip, deposited onto a commercial Si tip coated with NiCr. From this image, the radius is ≈5 nm and the cone angle 5°. The tip shows a resistance of $R \leq 1$ MΩ, which is sufficient for local oxidation.

standing sphere, whereas smaller spheres increase the local field underneath the tip. At this stage we do not consider the growing oxide itself as well as the focusing effect of the water layer or meniscus because of its large $\epsilon$. However, for an optimized focusing of the lateral fields, we would like to have a needle-like tip, which is still sufficiently conductive. So-called electron beam deposited (EBD) material is known to be suitable to define scanning tips with tip radii $\leq$5 nm and very small cone angles [12]. If deposited at high electron energies and low beam current densities, they appear to be conductive. Figure 6 shows an SEM image of an EBD tip deposited on top of an NiCr-coated Si tip. This tip shows an overall resistance $R \leq 1$ MΩ, which is sufficient for applications in electrochemical AFM and local oxidation and gives, in contrast to for example carbon nanotubes, the unique possibility to design the tip to exactly the requested geometry.

In summary, non-contact AFM has been used for locally oxidizing titanium thin films. In this mode, the tip–sample forces remain unchanged when a tip–sample bias is applied. This allows us to use oxide-sharpened Si tips, with which we are able to fabricate line grids with 6 nm structure sizes and 18 nm pitch. *In situ* electrical measurements give fine control over the lithographic process. In this way we fabricated tunnelling barriers as small as 15 nm. The current–voltage characteristic and the dependence of current on barrier width clearly indicate that tunnelling is the dominant transport mechanism in these devices. Numerical calculations of the lateral distribution of the tip-to-sample electric field indicate a further improvement in the lithographic resolution, if only needle-like tips with small radii and small cone angles are used. We show

that 5 nm radius, 5° cone angle EBD tips are sufficiently conductive to be used for local oxidation.

## References

[1] Dagata J A, Schneir J, Harary H H, Evans C J, Postek M T and Benett J 1990 *Appl. Phys. Lett.* **56** 2001
[2] Snow E S, Campbell F M and McMarr P J 1993 *Appl. Phys. Lett.* **63** 749
[3] Snow E S and Campbell P M 1994 *Appl. Phys. Lett.* **64** 1932
[4] Matsumoto K, Ishii M, Segawa K and Oka Y 1996 *Appl. Phys. Lett.* **68** 34
[5] Shen T-C, Wang C, Lyding J W and Tucker J R 1995 *Appl. Phys. Lett.* **66** 976
[6] Snow E S and Campbell P M 1995 *Science* **270** 1639
[7] Irmer B, Kehrle M, Lorenz H and Kotthaus J P 1997 *Appl. Phys. Lett.* **71** 1733
[8] Avouris P, Hertel T and Martel R 1997 *Appl. Phys. Lett.* **71** 285
[9] Sugimura H, UchidaT, Kitamura N and Masuhara H 1993 *Appl. Phys. Lett.* **63** 1288
[10] Ghandi S K 1983 *VLSI Fabrication Principles* (New York: Wiley)
[11] Lide D R (ed) 1992 *CRC Handbook of Chemistry and Physics* 72nd edn (Boston, MA: CRC)
[12] Wendel W, Lorenz H and Kotthaus J P 1995 *Appl. Phys. Lett.* **67** 3732